Rafael Duarte, Luís Moreira, Luís A. M. Barros, Vitor Monteiro, João L. Afonso, J. G. Pinto

"Power Converters for a Small Islanded Microgrid Based on a Micro Wind Turbine and an Battery Energy Storage System"

ECOS 31st International Conference on Efficiency, Cost, Optimization, Simulation and Environmental Impact of Energy Systems

ISBN: 978-972-99596-4-6

Rafael Duarte, Luís Moreira, Luís A. M. Barros, Vitor Monteiro, João L. Afonso, J. G. Pinto "Power Converters for a Small Islanded Microgrid Based on a Micro Wind Turbine and an Battery Energy Storage System", ECOS 31st International Conference on Efficiency, Cost, Optimization, Simulation and Environmental Impact of Energy Systems, pp.1-12, Guimarães, Portugal, June 2018. ISBN: 978-972-99596-4-6

Power Converters for a Small Islanded Microgrid Based on a Micro Wind Turbine and an Battery Energy Storage System

Rafael Duarte[a], Luís Moreira[a], Luís A. M. Barros[b], Vitor Monteiro[b], João L. Afonso[b], and J. G. Pinto[b]

[a] Centro ALGORITMI – University of Minho, Guimarães, Portugal, {a68538, a68531}@alunos.uminho.pt
[b] Centro ALGORITMI – University of Minho, Guimarães, Portugal, {luis.barros, vitor.monteiro, joao.l.afonso, gabriel.pinto}@algoritmi.uminho.pt

Abstract:

The growing awareness of the environmental issues has begun to change the traditional scheme of electric energy production along the last years, where fossil fuels based systems are a major cause for this change. For this reason, renewable energy sources are emerging as an ecologically way to produce energy. However, associated with the renewables integration into power grids, new challenges and opportunities arises. Although the crescent energy production, there are still 1.2 thousand million people without access to electricity, since some places are difficult to reach or is expensive to extend the power grid. As a contribution to solve this problem, this paper proposes a solution based on a Permanent Magnet Synchronous Generator (PMSG) micro wind turbine and a Battery Energy Storage System (BESS) to create an islanded microgrid. The developed and required power electronics hardware is presented and described in the paper, as well as the digital control platform, where is implemented the control system, with algorithms such as the Maximum Power Point Tracking (MPPT), used to extract the maximum power available at each instant in the micro wind turbine. A detailed analysis based on simulation results is presented and, aiming to verify the feasibility of the proposed solution, a laboratorial prototype was developed and experimental results in transient and steady state operation are presented and discussed in the paper.

Keywords:

Battery energy storage system, Islanded grid, Micro wind turbine, MPPT algorithm, Power electronics, Renewable energy sources.

1. Introduction

Electric energy has become an indispensable resource for humanity's needs. With the advancement in technology and population growth, it is predicted that the electric energy consumption continues growing. As can be expected, the traditional way of generating electrical energy with fossil fuels is no longer feasible, since the natural resources are limited and its usage has negative effects on the environment. One of the negative effects of this source is the emission of greenhouse gases, which 25% of them are produced by the electrical sector [1]. To overcome the demand in electric energy and mitigate the environment problems, renewables are emerging as promising sources of energy. Renewable energy sources are an ecologically viable alternative to fossil fuels, since its availability is large and its usage is cleaner. In this context, wind and solar energies are the ones that shows a greater growing in the last years [1]. These reasons lead to an increasing investment in these types of resources by some regions of the world, where the greater investment was in Europe, passing from 20.1% to 34.2% of electric power production based on renewable energy sources [1]. As example, in 2016, 55 GW of wind power capacity was added, making a global total wind power capacity of 487 GW [2][3], almost the double in relation to solar photovoltaic energy. Asia was responsible for half of the additions done during such year, being China the country with the most capacity added, reaching a total wind power capacity of 169 GW and representing one third of the global total wind

power capacity installed in 2016 [2][3]. Portugal is one of the European countries where is notorious an increasing wind power capacity in the last 10 years, having approximately 5.3 GW at the end of 2016, representing a share of nearly 24% of wind in the total gross electricity generation [4][5]. Despite the annual increase in power, there are still 1.2 billion people without access to electricity around the world. An example is India, where 24% of the population still does not have access to electricity, which is equivalent to 304 million people. Additionally, in sub-Saharan Africa, there are 622.6 million who do not have access to electricity [2][6]. To solve this problem, India has committed to give more emphasis to renewable energies and sub-Saharan Africa has committed to invest in microgrids using renewable energies.

As a contribution to the technological advancement and to mitigate the aforementioned problem, this paper presents a solution based on a Permanent Magnet Synchronous Generator (PMSG) micro wind turbine and a Battery Energy Storage System (BESS) to create an islanded microgrid. Along the paper, the development of the power electronic converters needed for the system is described, as well as the digital control platform used to implement all the control algorithms. A simulation model was implemented in PSIM software in order to obtain preliminary results for a better understanding of the proposed system. Aiming to verify the feasibility of the proposed system, a laboratorial prototype was developed and experimental results, in transient and steady state operation, are presented and discussed in the paper.

2. Theoretical Fundaments

To produce energy from wind it is necessary to use a Wind Energy Conversion System (WECS) known as wind turbine. Through the movement of its blades is produced mechanical energy which is after converted in electric energy by the electric generator. Depending on the application pretended for the system, the generated energy can be used to feed electrical appliances, stored in a BESS or injected into the Power Grid (PG).

2.1 Wind Power Extraction

The wind has a stochastic behavior, so there will be times the wind is available and others not. Furthermore, the production of energy by wind is affected by several factors, such as wind speed (v_w), air density (ρ), swept area of the rotor blades (A), generator electric efficiency (η_e) and mechanical efficiency (η_m) of components used [7]. The extraction of energy from the wind is done by the movement of the rotor blades, which turns kinetic energy into mechanical energy. This process ends lowering the wind speed that passes through the rotor blades. The more energy that is extracted, the lower the wind speed after the blades. However, extracting the maximum energy of the wind means nullifying its speed, but this is not possible, so another factor, known as power coefficient (C_p), must be considered to know the maximum energy that can be extracted with the wind turbine. As stated in [7] this power coefficient can only attain a maximum value of 59%, which is depicted as the Betz Limit. In practice, this value is situated between 40% and 50% for Horizontal Axis Wind Turbine (HAWT) and in 40% for Vertical Axis Wind Turbine (VAWT) [8]. Regarding the above statement, the power that can be extracted by the wind turbine from the wind follows (1). HAWT and VAWT are classified depending on its axis and structure [9].

$$P_{available} = \eta_e \eta_m \frac{1}{2} \rho A v_w^3 C_P \quad (1)$$

The VAWT presents some advantages as, e.g., allowing the generator and gearbox to be placed at the bottom of the tower, allowing an operation with every direction of the wind since a yaw system is not needed and allowing the wind turbine to be placed where the wind is turbulent. Nevertheless, this type of turbines presents lower efficiency relatively to HAWT since its Tip Speed Ratio (TSR) is limited [8][10][11]. The HAWT, contrarily to VAWT, have a rotation axis parallel to the ground and are noisier [7]. However, they operate at higher heights, allowing them to deal with less turbulent and more constant winds. Furthermore, HAWT have high efficiency relatively to their installation and maintenance costs [11]. Because of these features the market gained more interest in HAWT than in

VAWT, having in the last years a great development around HAWT leaving them with a share market of 99% and VAWT with 1% [7].

2.2 Wind Turbine Systems

WECS can be divided into islanded, connected to the PG and hybrid configurations. According to the application, the connection and components used are different, being necessary, in some cases, to add a BESS (islanded or hybrid system) [12]. There are situations where the connection with the PG is not possible or it is not the best choice, since its localization is difficult to reach or the costs are greater than implementing an islanded system. So, in this case, it is preferred an islanded system over one connected to the power grid. Fig. 1 shows a block diagram of an islanded system.

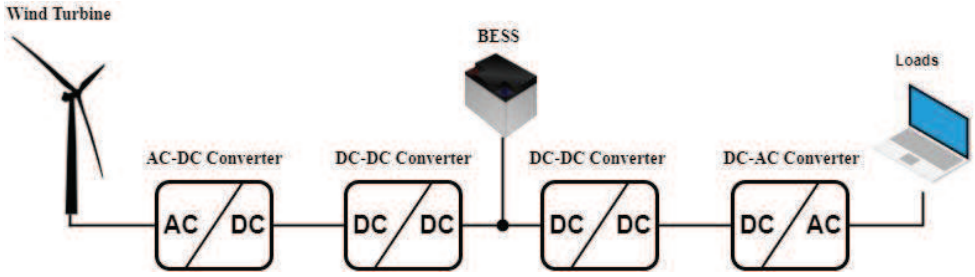

Fig. 1. Block diagram of a wind energy based islanded system.

As the wind has an intermittent behaviour, it is necessary to have a way to store energy in order to be able to feed the microgrid when the wind generator cannot produce energy due to the lack of wind. For that, it is essential to use a BESS. The types of converters used in this system are very similar to those used in power grid connected systems and in hybrid systems, consisting of a set of AC-DC, DC-DC and DC-AC converters, where the DC-DC should consider the BESS integration [12].

2.3 Energy Storage System

To reduce the harmful effects of energy production, other sources of renewable energy have been used. However, its intermittent nature introduces problems of stability, safety and electric power quality in the PG [13]. One way to solve this problem is to store the extracted energy for later usage through an Energy Storage System (ESS). There are several energy storage devices in the market today, such as batteries, inertia flywheels, fuel cells, flow batteries, supercapacitors, among others. The choice of an ESS for an application depends on several factors, such as the capacity, the power, the response time, weight, volume and operating temperature. However, there are two factors that characterize these energy storage technologies, which are the specific energy and specific power [13][14]. The specific energy is expressed in Wh/kg and represents the amount of energy that can be stored in the ESS, the specific power is expressed in W/kg and represents the rate at which the system can supply or receive energy. In the case of a battery, the power and energy capacities are highly dependent on the chemical used by the battery itself [14]. Among the various ESS, li-ion batteries were selected for the application proposed in this paper, since they have a good storage capacity, do not carry an environmental impact as high as lead-acid batteries and they have a low self-discharge.

2.4 MPPT Control Algorithms

As previously mentioned, the power extracted by the wind turbine is dependent of various factors, being some of them impossible to control (e.g., air density and wind velocity), controllable but only at manufacture (e.g., swept area of the rotor blades, mechanical and electric efficiencies) and controllable (e.g., Power coefficient (C_p)). The C_p is, at maximum, 59% and varies according to the pitch angle (β) and the Tip Speed Ratio (TSR) (λ), as can be seen in (2) [8], [15].

$$C_P(\lambda,\beta) = (0.44 - 0.0167\beta)sen\left(\frac{\pi\lambda}{4.775-0.3\beta}\right) - 0.0184\lambda\beta \quad (2)$$

By changing the pitch angle, the aerodynamic torque of the wind turbine is also changed. With that, it is possible to adjust the angle of attack of the rotor blades, and consequently, adjust the rotor speed.

The TSR is defined by the division of the tip speed of the rotor blades (v_t) by the wind speed (v_w). As can be seen in (3), the tip speed of the rotor blades depends on the rotation speed of the rotor (ω_m) and the radius of the rotor blades (R).

$$\lambda = \frac{v_t}{v_w} = \frac{\omega_m R}{v_w} \quad (3)$$

Changing the v_w or v_t induces other changes on the TSR, which varies the power coefficient. So, to maximize the power coefficient for each wind speed, the rotation speed of the wind turbine must be placed in a certain value. This can be seen in Fig. 2, where are identified the values of the rotation speed that maximizes the power extracted by the wind turbine for each wind speed.

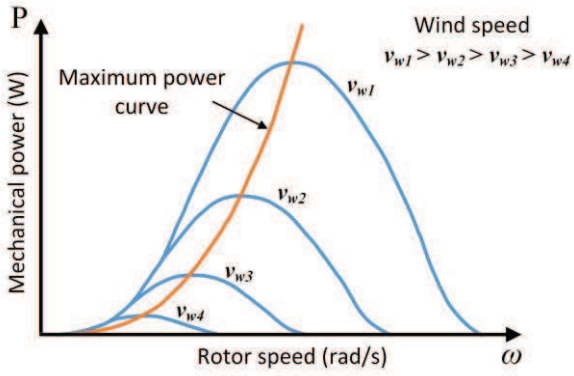

Fig. 2. Relationship between the rotation speed of rotor and mechanical power extracted (adapted from [15]*).*

During wind turbines operation to extract the maximum power available of the wind, is imperative to put some attention in some features of the wind turbine, such as the maximum rotation speed and the rated power of the wind turbine. So, when the rotor speed is below the rated speed, the turbine is controlled in order to operate with optimum TSR ($\lambda_{optimum}$). Conversely, when is superior, is controlled in order to maintain the rotor speed equal to its rated speed. Relatively to the rated power, when the wind turbine reaches this level, it is operated so the system continues to extract at maximum the rated power [15].

The control algorithms used to maximize the power extracted by the wind turbines are denominated as Maximum Power Point Tracking (MPPT) algorithms, and their effectiveness depends on the precision which they can monitor the maximum power point peaks [16]. Nowadays, there are a lot of MPPT algorithms and, most of them, can be divided in three categories: TSR control, Power Signal Feedback (PSF) and Perturbation and Observation (P&O) [16][17]. Between the three types of MPPT algorithms, the P&O is the cheapest, since it only needs to measure the current and voltage to calculate the electric power being extracted by the generator. On the other hand, the TSR control and PSF algorithms need additional sensors, like anemometers and tachometers. The P&O algorithm, also known as Hill-Climb Search, tries to put the system working near the maximum power point (MPP), oscillating around this point. Depending on the step size, this oscillation can be higher or smaller. With a small step the ripple is smaller, but the system takes more time to reach the MPP. With a larger step the ripple is higher, but the system reaches the MPP sooner. To mitigate both problems, a P&O algorithm with two modes was implemented: The fixed step mode and the adaptive step mode. At the beginning, the fixed step mode is enabled, allowing the system to reach more quickly the MPP. Once this point is reached, the P&O changes to the adaptive step mode in order to get more sensibility and to get closer to the MPP. Whenever the system detects a sudden variation, the fixed step mode is enabled again, repeating the process. In Fig. 3 is presented the flow chart of the implemented algorithm.

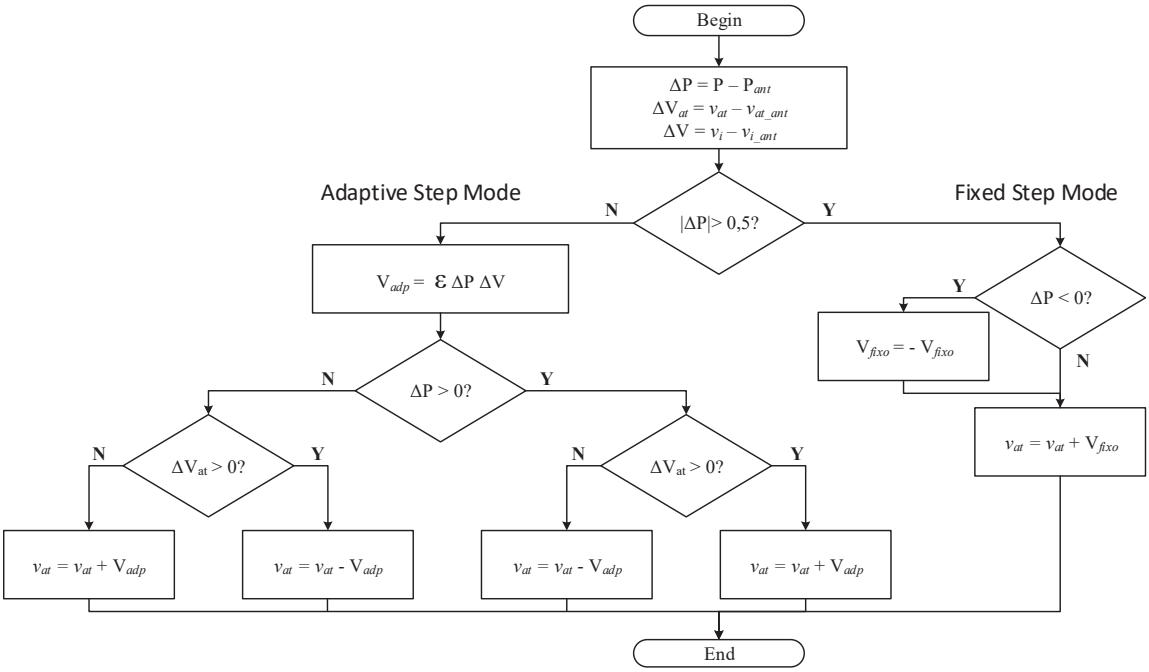

Fig. 3. Flow chart of the P&O algorithm with fixed and adaptive step modes [18].

3. Proposed Topology

The selected topology to interface the wind turbine generator and the islanded microgrid is shown in Fig. 4. The generator is a PMSG, composed by 6 pairs of poles produced by SilentWind. This generator has a nominal power of 450 W for a wind speed of 14.5 m/s and a nominal voltage of 24 V. Besides that, it has the versatility to operate at speeds ranging from 500 rpm. to 1700 rpm. and the minimum wind speed for the turbine to start operating is 2.2 m/s [19]. In order to adjust the alternating voltage from the PMSG into a DC voltage for the purpose of charging the BESS, an AC-DC followed by a DC-DC converter was implemented. At the AC-DC stage was chosen a non-controlled three-phase AC-DC converter due to its simplicity. The rectified output voltage from the AC-DC is used as input voltage for the DC-DC converter, where is interfaced the BESS. The BESS has a nominal voltage of 60 V, who is higher than the nominal voltage from the PMSG, therefore, a non-isolated boost DC-DC converter topology was chosen. Additionally, with the MPPT algorithm, the DC-DC converter is also responsible to extract the maximum power available from the wind turbine. Since the 60 V of the BESS is not enough to power-up the DC-AC converter used to create the microgrid, an additional DC-DC converter should be used between the DC-DC and the DC-AC.

The rated power of the wind turbine is 450 W, but the system has been designed to feed loads up to 1 kVA, so the use of non-isolated DC-DC converters is not adequate for this application. In terms of isolated topologies, there are some variants, such as forward converters (single-switch and dual-switch), push-pull, half-bridge, and full-bridge. Among all these derivations, the full-bridge is the one that has greater capacity to deal with high powers, being for this reason, used extensively in applications of medium and high power conversion [20]. In addition, the ripple of the output voltage is smaller, since the resulting wave of rectification on the secondary side of the transformer becomes double the frequency, which ends up reducing significantly the harmonic content. This has the advantage of allowing a smaller passive filter to be used at the output. For these reasons, the full-bridge DC-DC bridge converter was chosen to provide a 400 V DC bus, capable of powering the DC-AC converter and enabling it to create a 230 V single-phase grid.

Finally, for the microgrid implementation, a single-phase full-bridge converter was selected, since it is a simple topology to control and implement. In conjunction with this converter, a LC low-pass passive filter was adopted, which is capable of attenuating the high-frequency harmonics present in the output waveform of the DC-AC converter. This single-phase full-bridge converter must be capable of generating an output voltage with a fixed amplitude and frequency, as well as a low

harmonic distortion, regardless of the type of load to be supplied (linear or non-linear). For this, the control technique to be implemented is based on a PI controller.

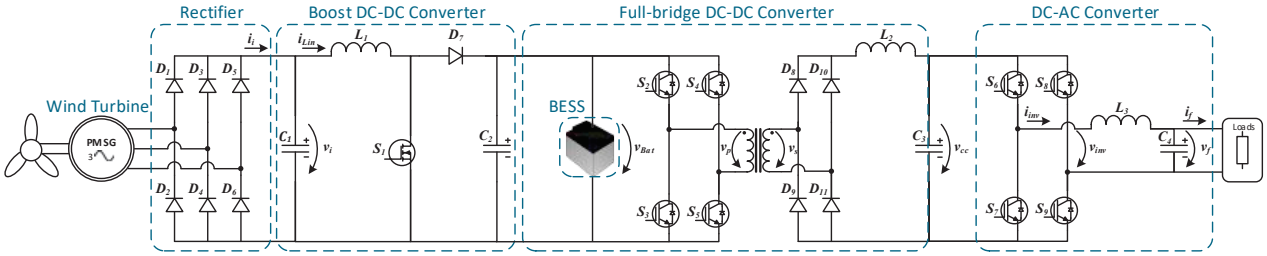

Fig. 4. Topology chosen to interface a micro wind turbine with an islanded microgrid.

4. Simulation Results

Considering the selected topology, an analysis was performed through a dedicated simulation software for power electronics (PSIM). The more relevant simulation results are presented in detail along this section.

4.1 Micro Wind Turbine

The element that feeds the entire system from the wind is the micro wind turbine, so this element is essential for understanding and designing the entire system. As previously mentioned, the micro wind turbine extracts the energy available in the wind by moving the rotor and the electric generator. This whole process can be modelled in a simulation environment, allowing to change the parameters in a simple way and presenting a robust interface. Fig. 5 shows the power curve obtained with the simulation model. The wind turbine modelled was the 24 V design made by SilentWind, and, as can be seen, the simulation model slightly exceeds the power of 450 W, being close to 460.5 W. However, reaching this value with a rotor speed of 1696 rpm. and with a generator output voltage of 56.2 V (similar to the specified in the 24 V, 1700 rpm., 57 V model).

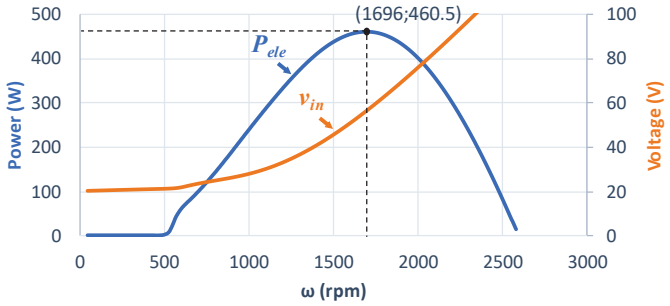

Fig. 5. Power curve of the modelled wind turbine in PSIM.

4.2 MPPT Algorithm

The DC-DC converter used between the PMSG and the BESS is responsible of implementing the MPPT algorithm. During the tests of the micro wind turbine model provided by PSIM it was noted that, due to the moment of inertia of the turbine being relatively high, its response to wind variations was not instantaneous. For this reason, the sampling of the extracted power was done at a frequency of 10 Hz, since with a higher frequency the readings obtained no longer corresponded to the result of the actuation. The measured power, sampled at 10 Hz, results from the multiplication between the current in the inductance and the input voltage of the boost DC-DC converter. These two values (current and voltage) are sampled at 50 kHz and the result of the multiplication is used as input for a low-pass digital filter. In this way, power peaks that may occur due to noise in the sensor readings are attenuated.

In Fig. 6 is shown the operation of the MPPT algorithm for different wind speeds. Initially the wind (v_w) has a value of 14.5 m/s and as the generator is still starting it takes approximately 2.3 s to reach

the maximum power point (P_{max}). After that, the power variations are smaller, since the increment becomes adaptive. Therefore, it can be concluded that the algorithm can reach, in a short time, the maximum power and maintain a minimum variation over the time. After 4 s, the wind begins to slow down to 8 m/s. At this point, the maximum power is approximately 87 W and the algorithm takes less time (about 1.8 s) to put the generator extracting that power. At 6.2 s, the wind speed increases to 10 m/s and the maximum power reaches 165 W. As the speed difference is not so great, the controller took only 1.2 s to reach the point of maximum power. Finally, at 9.5 s, the wind speed returns to 14.5 m/s, now taking 1.2 s to starts extracting 460.5 W.

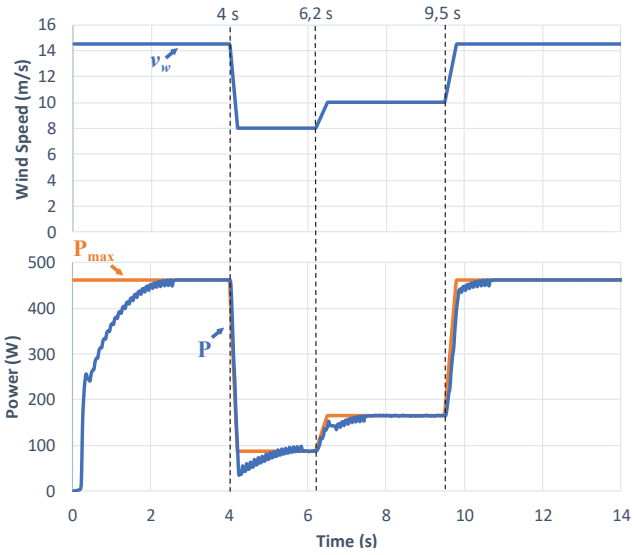

Fig. 6. Extracted power and maximum power available according to wind speed.

4.3 DC Bus Voltage Control

To maintain a regulated 400 V on the DC bus, a PI controller was implemented in the full-bridge converter. The modulation used in such converter was the phase-shift modulation, where both legs (leading leg and lagging leg) are controlled with a duty-cycle of 50% and with a phase change between them [20]. The value of the leading or lagging phase determines how much power is transferred from the BESS to the DC bus of the DC-AC converter. In order to test the full-bridge DC-DC converter, a 550 W load was placed in parallel with the 400 V DC bus and the BESS voltage was changed. As can be seen in Fig. 7, the PI controller applied in the converter can regulate the DC bus of the DC-AC converter at 400 V. At the beginning, the controller applied the maximum phase angle (approximately 81º) and the voltage of the DC bus increased almost instantaneously to 400 V. After that, the phase angle varied and then stabilized in the angle needed to maintain the voltage at 400 V, which in this case was near 75º. However, at 400 ms the BESS voltage started falling, and to keep the DC bus at 400 V, the phase angle had to be greater, keeping that way the power that was delivered to the DC bus. At 800 ms, the BESS voltage reaches 60 V and the phase angle stabilized at 80º, maintaining the DC bus voltage at 400 V.The DC bus of the DC-AC converter reached 400 V in less than 300 ms, but the initial current required for that was too high, reaching 166 A (Fig. 8(a)). Considering this high value of current, the components used would end being destroyed. To prevent that, the initially power transferred needs to be lower, therefore, the phase angle should be lower. When the DC bus reaches a certain voltage, the PI controller is activated and from there on, the DC bus is regulated at 400 V, but without needing a high current. Due to this, the converter takes more time to reach 400 V, since the energy transferred initially is less than before.

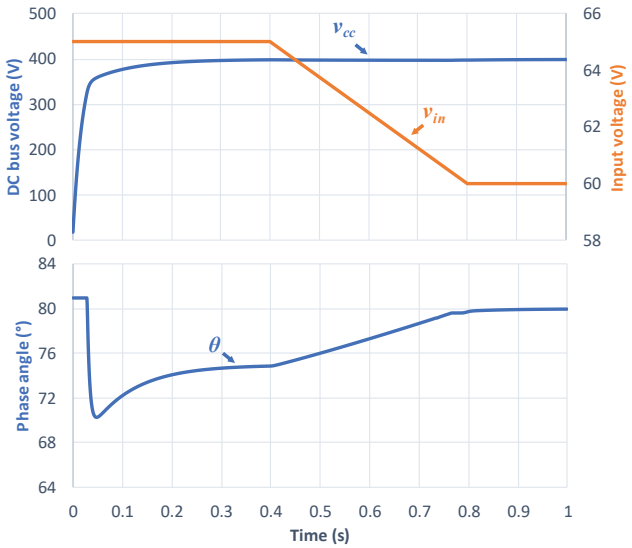

Fig. 7. Phase angle variation to regulate the DC bus due to BESS voltage chances

As can be seen in Fig. 8(b), applying a pre-charge strategy, the converters takes 5.8 s to charge the DC bus with 400 V. Regarding this, the converter is initially operated with a phase angle of 9º until the DC bus assumes a voltage of 100 V. Then, the phase angle is changed to 36º, letting the DC bus charge faster than before. At 390 V, the PI controller is activated and, since the DC bus is closer to 400 V, the converter takes a few milliseconds to regulate the DC bus at 400 V.

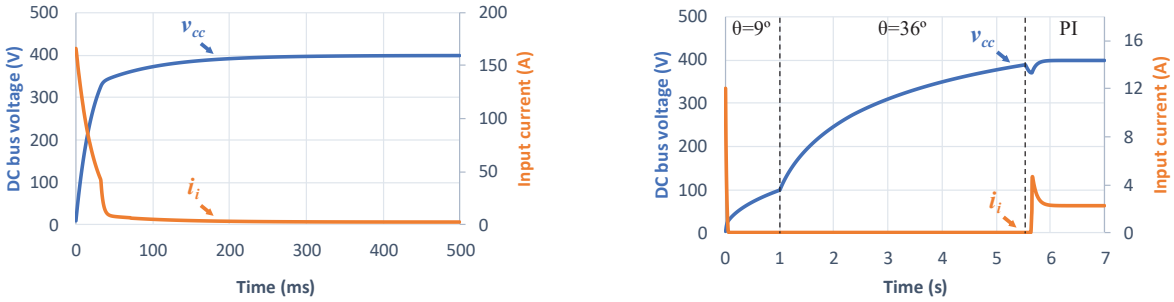

Fig. 8. Maximum current needed to regulate the DC bus: (a) With pre-charge; (b) Without pre-charge.

4.4 DC-AC Converter

As aforementioned, the DC-AC converter should be controlled to generate a sinusoidal waveform with nominal values of 230 V RMS voltage and frequency of 50 Hz. Moreover, it should present a Total Harmonic Distortion (THD) lower than 5% to accomplish the IEEE Standard 519-2014 [21]. Regarding that, a simulation model was developed, consisting of two stages: a DC-AC converter and a low-pass filter. The power converter is responsible of generating the signals needed to establish the single-phase power grid voltage with the required frequency, while the filter is responsible of attenuating the high-frequency harmonics resulting from the semiconductor switching. Taking into account that the linear and non-linear loads can be connected to the DC-AC converter, a set of simulation tests were carried out, aiming to analyse the DC-AC converter behaviour. As initial test, a linear load of 600 W (consisting in a resistance of 88 Ω) was used. Since this is a linear load, the current THD is equal to the THD of the voltage produced by the DC-AC converter. Therefore, if the produced voltage has a low value of THD, then, the current also has a low value of THD. As can be seen in Fig. 9(a), the results obtained are quite satisfactory with a voltage THD of 0.48%. As expected, the produced voltage has a RMS voltage value of 229 V and a frequency of 50 Hz. With a non-linear load, the distortion of the current no longer depends on the applied voltage, so even if the load voltage has a low value of THD, the current value of THD still exists. For this reason, the current passing

through the inductance of the low-pass filter will cause a voltage drop that will distort the voltage in the load, therefore, the algorithm will have to be able to compensate this effect. By compensating these distortions, caused by the voltage drop in the inductance, the load is supplied with an acceptable sinusoidal voltage, although it consumes a rather distorted current. As shown in Fig. 9(b), for a non-linear load, the produced voltage has a THD value of 0.48% and the current consumed by the non-linear load has a THD value of 158%.

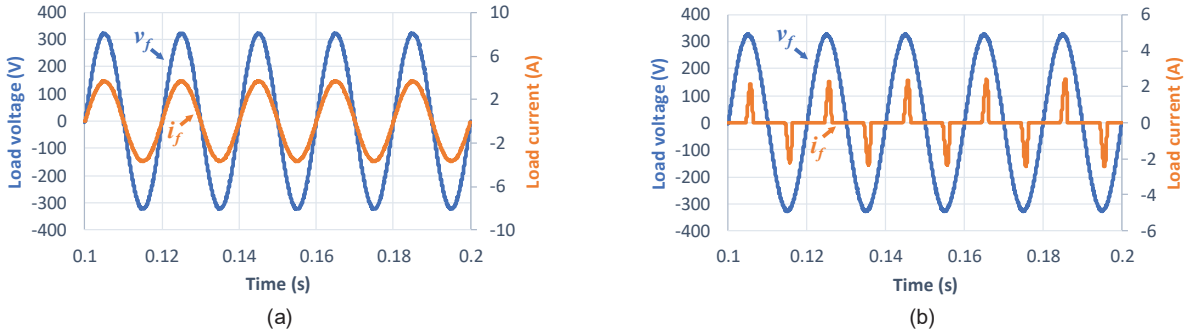

Fig. 9. Voltage and current delivered by the DC-AC converter when supplying: (a) Linear load; (b) Non-linear load.

5. Implementation and Results

Aiming to verify the feasibility of the proposed solution, a laboratorial prototype was developed and several experimental results were obtained, some of them are presented and discussed in this section. The developed system consists of two main parts, the test bench and the laboratory prototype. The test bench has the purpose of emulating the wind behaviour and is composed by a three-phase squirrel cage induction motor, controlled by a variable speed drive, coupled to the PMSG. On the other hand, the laboratorial prototype is composed by the control circuit (including control boards and a digital signal processor where the control algorithms are implemented), by the power circuit (including the different power converters), and by the BESS. Fig. 10 shows the workbench used to obtain the experimental results.

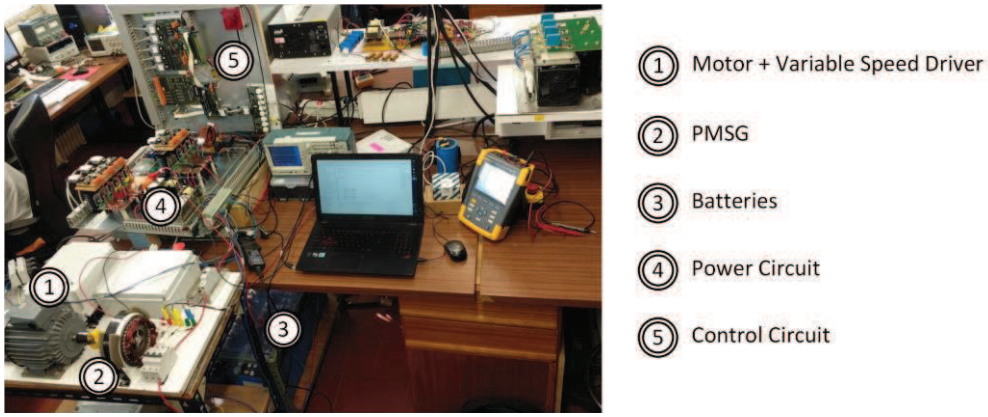

Fig. 10. Laboratory workbench used to test the prototype of the proposed solution.

As aforementioned, with the addition of BESS, the developed system can operate as an islanded microgrid. For the safety of the equipment used, the system was tested with a RMS voltage of 115 V. To verify the correct operation of the two power converters after the DC bus of the BESS, the full-bridge DC-DC converter was controlled to regulate the DC bus of the DC-AC converter at 220 V and the output of the DC-AC converter coupled to a resistive load of 78 Ω. Fig. 11 (a) shows the experimental results obtained with a linear load (resistance of 78 Ω). As can be seen, not only the DC bus is regulated at 220 V, but also the load was supplied with a RMS voltage of 115 V and with a THD value of 1.1%. In this case, the measured current has a value of 1.41 A and the BESS voltage has a value of 37 V. On the other hand, Fig. 11(b) shows the experimental results obtained with a

non-linear load (composed by a rectifier with an AC inductor of 5.17 mH and with a DC shunt association of a capacitor of 470 µF with a resistor of 130 Ω). As can be seen, the DC bus is regulated at 220 V, the produced voltage has a nominal value of 115 V and a frequency of 50 Hz, and the consumed current has a value of 2.32 A. In this case, the THD of the produced voltage raised to 1.5%, but within the IEEE standards is acceptable.

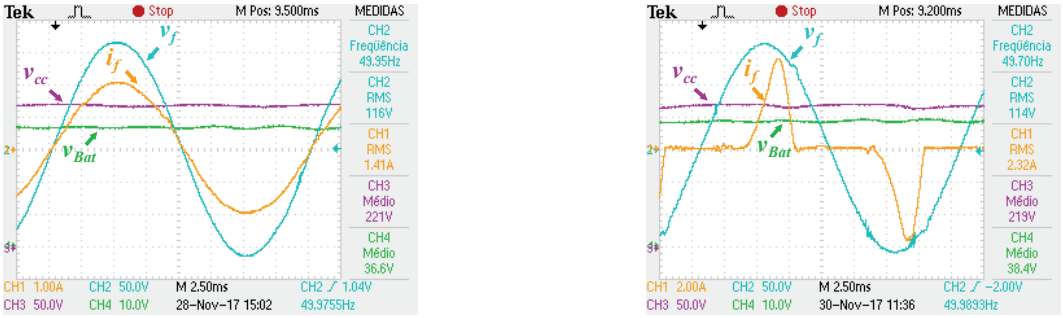

Fig. 11. Experimental results obtained when the DC bus is regulated at 220 V and the DC-AC converter is establishing a microgrid with a RMS voltage of 115 V: (a) Feeding a resistive load of 78 Ω; (b) Feeding a non-linear load composed of a rectifier type with capacitive filter.

Regarding the validation of the MPPT algorithm implemented, the boost DC-DC converter was controlled to extract continuously a current of 1 A from the generator of the wind turbine. As shown in Fig. 12, the DC-AC converter could supply a resistive load of 130 Ω with 115 V even when the BESS is receiving energy from the Boost DC-DC converter. Therefore, it was possible to verify that the prototype can establish an adequate voltage for linear or non-linear loads, even when the BESS is receiving energy from the generator of the wind turbine.

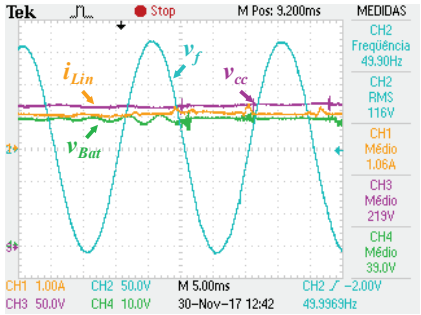

Fig. 12. Experimental results obtained when the DC bus is regulated at 220 V, the DC-AC converter is establishing a microgrid with a RMS voltage of 115 V and the Boost DC-DC converter extracts continuously 1 A from the generator.

In order to verify the operation of the MPPT algorithm a system composed by a rheostat in series with a DC power supply was used. According to the maximum power transfer theorem [22], in a resistive circuit, for the algorithm to be able to extract the maximum power available from the DC source, the DC-DC converter should be able to equal the resistance imposed by the rheostat. So, with a DC source of 20 V, the voltage of the converter and the voltage of the rheostat should be equal to 10 V to prove that the MPPT algorithm implemented is extracting the maximum power available. Observing Fig. 13(a), it is verified that the MPPT algorithm took 2 s to reach the MPP. After that, the algorithm changes to adaptive step mode and started getting gradually closer to the MPP with a smaller ripple. When the steady-state was reached, the voltages of the power converter and the rheostat were practically the same, so it was proven that the MPPT algorithm was working as expected. For this test, the resistance of the rheostat was fixed at 17 Ω, but for Fig. 13 (b), the resistance was changed from 10 Ω to 7 Ω and then to 13.5 Ω. Analysing the obtained results, it is verified that after 2.5 s, the algorithm was activated and after a short time the system could reach the

MPP, drawing a power near to 37 W. After 10 s, the resistance of the rheostat was set at 7 Ω and the MPPT algorithm responded immediately to that variation, putting the converter extracting about 52 W. Finally, at 17.5 s, the load of the rheostat was changed again, being now 13.5 Ω and the system almost immediately reached the maximum power point and started extracting, approximately, 30 W. With this, it is possible to conclude that the MPPT algorithm worked properly and that its response time to variations was quite fast.

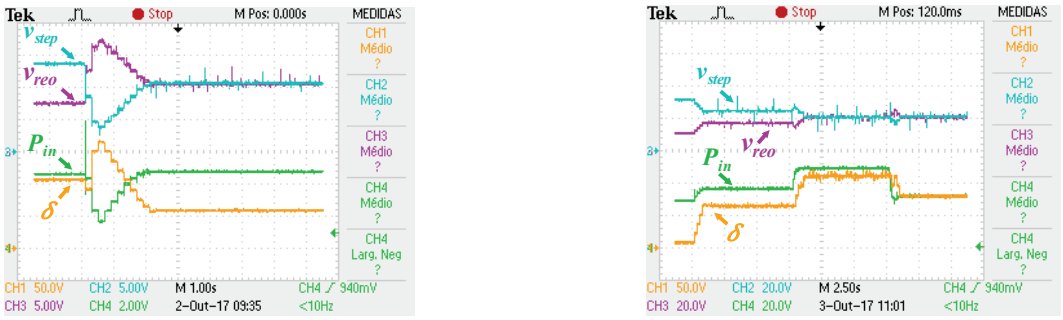

Fig. 13. Experimental results obtained during the tests of the MPPT algorithm: (a) Fixed resistance; (b) Variable resistance.

6. Conclusions

This paper proposes a solution based on a Permanent Magnet Synchronous Generator (PMSG) micro wind turbine and a Battery Energy Storage System (BESS) to create an islanded microgrid. The proposed system should be able to extract the maximum power available at any instant from the wind turbine and store it in the BESS. Besides, it should be able of supplying linear and non-linear electrical loads. A laboratorial prototype was developed and the obtained results shows that the proposed system operates as expected, i.e., the boost DC-DC converter is able of putting the prototype working at the MPP, the full-bridge DC-DC converter is able to regulate the DC bus voltage of the DC-AC converter, and the DC-AC converter is suitable to generate a voltage with the desired frequency and amplitude with low value of total harmonic distortion.

Acknowledgments

This work has been supported by COMPETE: POCI-01-0145-FEDER-007043 and by FCT within the Project Scope: UID/CEC/00319/2013. This work is financed by the ERDF – COMPETE 2020 Programme, and FCT within project SAICTPAC/0004/2015- POCI- 01-0145-FEDER-016434.

7. References

[1] World Energy Council, "World Energy Resources | 2016," *World Energy Council*, 2016. [Online]. Available: https://www.worldenergy.org/wp-content/uploads/2016/10/World-Energy-Resources-Full-report-2016.10.03.pdf. [Accessed: 24-Sep-2017].

[2] REN21, "Renewables 2017 global status report 2017," 2017. [Online]. Available: http://www.ren21.net/wp-content/uploads/2017/06/17-8399_GSR_2017_Full_Report_0621_Opt.pdf. [Accessed: 16-Sep-2017].

[3] GWEC, "Global Wind Report - Annual Market update 2016," 2016. [Online]. Available: http://www.indianwindpower.com/pdf/GWEC_Global_Wind_2016_Report.pdf. [Accessed: 23-Sep-2017].

[4] APREN; INEGI, "Parques Eólicos em Portugal Wind Farms in Portugal," *APREN; INEGI*, 2016. [Online]. Available: http://e2p.inegi.up.pt/relatorios/Portugal_Parques_Eolicos_2016.pdf. [Accessed: 23-Sep-2017].

[5] REN, "Dados Técnicos 2016 - Technical Data," *Redes energéticas Nacionais, SGPS, S.A*, 2016. [Online]. Available: https://www.ren.pt/files/2017-03/2017-03-24140032_7a820a40-

3b49-417f-a962-6c4d7f037353$$7319a1b4-3b92-4c81-98d7-fea4bfefafcd$$912d7292-4d3c-4faa-8a0b-2f750e707e15$$File$$pt$$1.pdf. [Accessed: 19-Sep-2017].

[6] Washington Post, "Without electricity, 1.3 billion are living in the dark - Washington Post." [Online]. Available: https://www.washingtonpost.com/graphics/world/world-without-power/?hpid=hp_no-name_graphic-story-b%3Ahomepage%2Fstory. [Accessed: 01-Nov-2016].

[7] ABB, "Technical Application Papers No.13 : Wind power plants," no. 13, p. 123, 2011.

[8] S. ERIKSSON, H. BERNHOFF, and M. LEIJON, "Evaluation of different turbine concepts for wind power," *Renew. Sustain. Energy Rev.*, vol. 12, no. 5, pp. 1419–1434, Jun. 2008. doi: 10.1016/j.rser.2006.05.017, ISSN: 13640321.

[9] D. A. Spera, *Wind Turbine Technology: Fundamental Concepts in Wind Turbine Engineering*, vol. 62. Three Park Avenue New York, NY 10016-5990: ASME, 2009. doi: 10.1115/1.802601, ISSN: 0038092X.

[10] E. W. E. Association, *Wind Energy-- the Facts: A Guide to the Technology, Economics and Future of Wind Power*, 1st editio. Routledge, 2009. doi: ISBN: 9781849773782.

[11] J. Bukala, K. Damaziak, H. R. Karimi, K. Kroszczynski, M. Krzeszowiec, and J. Malachowski, "Modern small wind turbine design solutions comparison in terms of estimated cost to energy output ratio," *Renew. Energy*, vol. 83, pp. 1166–1173, Nov. 2015. doi: 10.1016/j.renene.2015.05.047, ISSN: 18790682.

[12] R. Dutra, "Energia Eólica: Princípios e Tecnologia," 2008. [Online]. Available: http://www.cresesb.cepel.br/download/tutorial/tutorial_eolica_2008_e-book.pdf. [Accessed: 13-Nov-2016].

[13] S. Vazquez, S. M. Lukic, E. Galvan, L. G. Franquelo, and J. M. Carrasco, "Energy storage systems for transport and grid applications," *IEEE Trans. Ind. Electron.*, vol. 57, no. 12, pp. 3881–3895, Dec. 2010. doi: 10.1109/TIE.2010.2076414, ISSN: 02780046.

[14] N. Miller, D. Manz, J. Roedel, P. Marken, and E. Kronbeck, "Utility scale Battery Energy Storage Systems," in *IEEE PES General Meeting*, 2010, pp. 1–7. doi: 10.1109/PES.2010.5589871.

[15] M. Karbakhsh, H. Abutorabi, and A. Khazaee, "An enhanced MPPT fuzzy control of a wind turbine equipped with permanent magnet synchronous generator," *2012 2nd Int. eConference Comput. Knowl. Eng.*, pp. 77–82, Oct. 2012. doi: 10.1109/ICCKE.2012.6395356.

[16] J. Singh and M. Ouhrouche, "MPPT Control Methods in Wind Energy Conversion Systems," in *Fundamental and Advanced Topics in Wind Power*, InTech, 2011, p. 23. doi: 10.5772/21657, ISSN: 978-953-307-508-2.

[17] M. Rolak, R. Kot, M. Malinowski, Z. Goryca, and J. T. Szuster, "Design of Small Wind Turbine with Maximum Power Point Tracking Algorithm," in *2011 IEEE International Symposium on Industrial Electronics*, 2011, pp. 1023–1028. doi:10.1109/ISIE.2011.5984300.

[18] M. Ceretta Moreira, D. Lellis Hoss, M. Jinbo, F. A. Farret, and G. Cardoso Junior, "Fixed and Adaptive Step HCC Algorithms for MPPT of the Cylinders of Magnus Wind Turbines," in *3rd Renewable Power Generation Conference (RPG 2014)*, 2014, p. 8.36-8.36. doi: 10.1049/cp.2014.0921.

[19] SilentWind, "Manual Aerogeradores SILENTWIND," 2010. [Online]. Available: http://www.silentwindgenerator.com/themes/regular/silentwind/images/prodimgs/10/icon1_pt_10.pdf?v=1500829578. [Accessed: 23-Jul-2017].

[20] X. Ruan, *Soft-Switching PWM Full-Bridge Converters*. Singapore: John Wiley & Sons, Ltd, 2014. doi: 10.1002/9781118702215.

[21] IEEE, *IEEE Recommended Practices and Requirements for Harmonic Control in Electrical Power Systems*. 2014. doi: 10.1109/IEEESTD.2014.6826459.

[22] K. V. Cartwright, "Non-Calculus Derivation of the Maximum Power Transfer Theorem," in *Citeseer*, 2008, pp. 1–19.